Journal of
Manufacturing and Materials Processing

MDPI

Article

Optimization of the Operating Behavior of Spur Gears Through Machine Hammer Peening

Mohammad Dadgar [1], Sebastian Sklenak [2], Martina Müller [1], Tim Herrig [1,*], René Greschert [2], Dieter Mevissen [2], Christian Brecher [2,3] and Thomas Bergs [1,3]

[1] Manufacturing Technology Institute (MTI), RWTH Aachen University, Campus-Boulevard 30, 52074 Aachen, Germany; mohammad.dadgar@rwth-aachen.de (M.D.); m.mueller@mti.rwth-aachen.de (M.M.); t.bergs@mti.rwth-aachen.de (T.B.)
[2] Laboratory for Machine Tools and Production Engineering (WZL), RWTH Aachen University, Steinbachstr. 19, 52074 Aachen, Germany; s.sklenak@wzl.rwth-aachen.de (S.S.); d.mevissen@wzl.rwth-aachen.de (D.M.); c.brecher@wzl.rwth-aachen.de (C.B.)
[3] Fraunhofer Institute for Production Technology (IPT), Steinbachstr. 17, 52074 Aachen, Germany
* Correspondence: t.herrig@mti.rwth-aachen.de

Abstract

Gear systems operate under high mechanical and tribological loads, making their surfaces vulnerable to wear and fatigue. Improving surface durability requires finishing processes that improve near-surface properties and extend service life. Since machine hammer peening (MHP) offers such potential, this study investigates its influence on the performance of case-hardened spur gears and evaluates its suitability as an alternative to shot peening as a conventional finishing method. Analog specimens with simplified geometries were treated using various MHP parameters to identify effective process settings. These optimized settings were then applied to real spur gears to assess performance under practical conditions. The experiments showed that MHP can significantly modify surface integrity, achieving surface roughness reductions of up to 55%, surface hardness increases of up to 30%, and compressive residual stresses exceeding −1400 MPa with stability to depths of 200 µm. These modifications resulted in improved wear and fatigue performance, with increases in load cycle number in the tooth flank up to 99% and an increase in load amplitude in the tooth root of more than 5%. For comparison, specimens were also treated with shot peening. Although MHP induced stronger surface integrity modifications, shot peening achieved higher overall load-carrying capacity because several critical areas could not be fully accessed by MHP, limiting its effectiveness. Overall, MHP shows promise as a finishing process, but its full potential depends on overcoming accessibility limitations in complex gear geometries.

Keywords: machine hammer peening; spur gears; surface structuring; roughness; hardness; residual stresses

Check for updates

Academic Editor: Tuğrul Özel

Received: 20 January 2026
Revised: 20 February 2026
Accepted: 23 February 2026
Published: 26 February 2026

1. Introduction

Spur gears are essential components in mechanical power transmission systems and are subjected to continuous mechanical and tribological loads during operation. These demanding service conditions can lead to a variety of damage mechanisms and failure modes that limit gear lifetime and reliability. Typical gear damages include wear caused by material removal at the tooth flanks, plastic deformation under high contact stresses, contact fatigue under cyclic loading manifested as micro pitting and pitting, crack initiation and propagation at highly stressed regions such as the tooth root, scuffing resulting from excessive friction and inadequate lubrication, and ultimately tooth breakage under severe operating conditions or in the presence of manufacturing-related defects [1–5]. Together, these damage mechanisms and failure modes highlight the critical role of appropriate remedial measures in improving the durability and load-carrying capacity of spur gears [6,7].

To mitigate damage mechanisms and delay failure in gears, various remedial strategies have been developed, which can be broadly classified into heat treatments and complementary surface treatments [8]. Conventional heat treatments for gears include induction hardening and case hardening [9]. Induction hardening employs electromagnetic induction to heat the gear, followed by rapid cooling to increase hardness and fatigue resistance [10]. Case hardening involves the diffusion of carbon or nitrogen into the surface, producing hard, wear-resistant layer while maintaining a ductile core [11]. Surface treatments offer a complementary approach by directly modifying the near-surface region, which is critical for tribological performance and fatigue resistance [5]. A widely investigated method is laser surface texturing [12], in which laser structuring is used to create micro-lubricant pockets [13] that enhance lubrication preservation and reduce the entry of wear particles into the contact zone [14]. Furthermore, laser texturing has also been reported as beneficial for improving the performance of functional coatings [15], which can significantly enhance wear resistance, pitting resistance and overall load-carrying capacity of gears [16]. Moreover, laser shock peening employs high-energy laser pulses to generate shock waves that induce deep compressive residual stresses, thereby enhancing fatigue resistance and preventing crack propagation [17]. However, laser-based methods may introduce thermal residual stresses [18] or localized melting, which can promote crack initiation [19]. For this reason, forming-based surface treatments have gained increasing attention due to their ability to induce compressive residual stresses and work hardening without significant thermal influence [20]. Among these methods, shot peening is widely used to strengthen gear surfaces through high-velocity particle impacts, resulting in beneficial compressive residual stresses and improved fatigue life [21]. Machine hammer peening (MHP) has recently been identified as a promising alternative forming-based surface treatment process [22]. The main remedial strategies discussed above are schematically summarized in Figure 1.

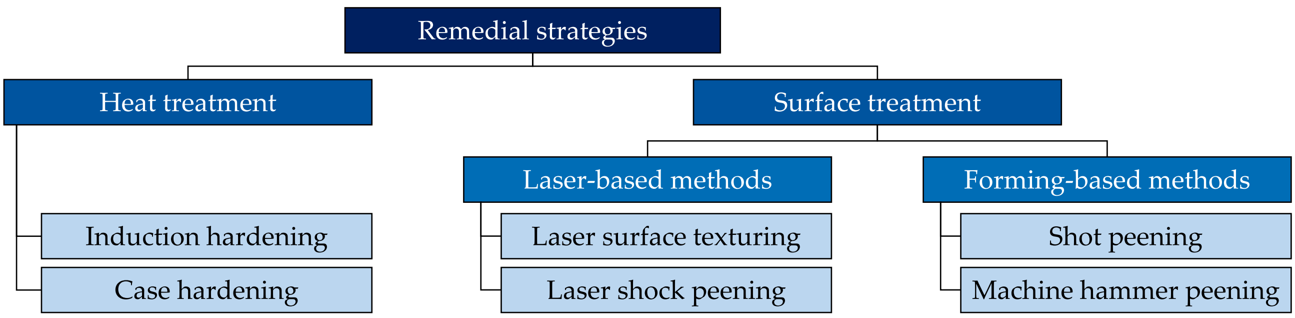

Figure 1. Schematic overview of common remedial strategies for improving the resistance of gears to damage and failure, including heat treatment and surface treatment.

MHP employs a high-frequency impact mechanism driven by an actuator-controlled plunger [23], producing localized plastic deformation in the near-surface layer [24]. As a result, MHP can smooth the surface [25], increase hardness [26], induce compressive residual stresses [27], and modify microstructural features [28]. As a cold-forming process, MHP does not introduce thermal residual stresses or unwanted thermal effects, similar to shot peening. A distinctive advantage of MHP is its ability to generate comparatively uniform surface conditions while simultaneously reducing surface roughness, whereas conventional shot peening often leads to increased roughness [22]. This characteristic is particularly relevant for gear applications, where improved frictional behavior is essential for mitigating wear under rolling-sliding contact conditions.

Studies on the behavior of gears have shown that compressive residual stresses play a crucial role in increasing fatigue resistance by delaying crack initiation and slowing crack propagation [29]. Investigations on analog gear specimens further demonstrated that MHP can increase pitting resistance through the combined effects of surface smoothing, micro-structuring, and high compressive residual stresses [30]. However, these findings focus on tooth flank behavior, whereas the influence of MHP on tooth root fatigue remains unexplored. Since flank and root failures arise from distinct mechanisms, the application of MHP to gears requires managing competing process requirements. Moderate energy input is favorable for tribological performance on tooth flanks, whereas higher energy levels are necessary to generate the compressive stresses required for root strengthening [31]. Furthermore, although the effects of MHP on simplified geometries have been investigated to some extent [32,33], a comprehensive study on real gears, whose complex geometries restrict hammer accessibility, is still lacking.

To address these gaps, the aim of this study is to understand how MHP influences both the surface integrity and load-carrying capacity of spur gears. First, the influence of different MHP parameter settings on surface integrity is evaluated. The resulting findings then serve as the basis for analyzing fatigue performance. Moreover, since shot peening represents the conventional finishing process for gears, direct comparisons are conducted to more clearly assess the capabilities and limitations of MHP relative to shot peening. Overall, this study provides a comprehensive assessment of how MHP modifies key surface integrity characteristics and the load-carrying capacity of gears, and it highlights the geometric constraints that must be overcome for successful industrial application of the process.

2. Materials and Methods

This study employs an experimental approach to investigate the influence of MHP on the surface integrity and load-carrying capacity of spur gears under representative manufacturing and service-relevant conditions. To achieve this, two types of components with different geometrical complexity were manufactured at the authors' facilities using raw material supplied by Ovako (Stockholm, Sweden) and subsequently investigated. First, cylindrical analog shafts with simplified geometry were used for initial experiments to enable a controlled investigation of MHP effects under well-accessible conditions, as shown in Figure 2a. These comprised counter shafts made of 16MnCr5 and test shafts made of 18CrNiMo7-6, produced through a process chain including pre-turning, stress-relief annealing, finishing turning, case hardening, and grinding. Second, real spur gears with geometrically complex tooth flanks and tooth roots, made of 18CrNiMo7-6, were investigated to assess the applicability and accessibility of MHP to critical functional surfaces under realistic component-level conditions, as shown in Figure 2b. The gears were assessed in the as-milled condition, reflecting typical industrial boundary conditions before surface finishing.

MHP was performed using an Accurapuls hammer system mounted on an ABB industrial robot, with the specimens positioned on the external rotation axis, as shown in Figure 3a. The MHP process parameters included a hammer frequency of f = 120 Hz, a stepover distance of s = 0.07 mm, a stroke distance of h = 0.3 mm, and a hammerhead diameter of d = 8 mm, selected based on previous work [31]. A spiral-like hammering strategy was employed because it prevents repeated peening of the same location and avoids abrupt directional changes [4], as illustrated in Figure 3b. In real spur gears, neighboring teeth restrict accessibility to the tooth root and flank, which limits machining orientations and requires different combinations of impact angle and machining direction depending on local geometry. To systematically study these effects, the MHP impact angle was varied at β_i = 15°, 30°, and 45°, and each angle was tested in both pushing and pulling directions, resulting in six distinct MHP setups, as summarized in Table 1. Tests on cylindrical analog specimens examined how impact angle and machining direction influence surface topography and subsurface characteristics by modifying roughness, hardness, and residual stresses. These results were then used to identify parameter combinations that produce tribologically favorable surface structures with high compressive residual stresses.

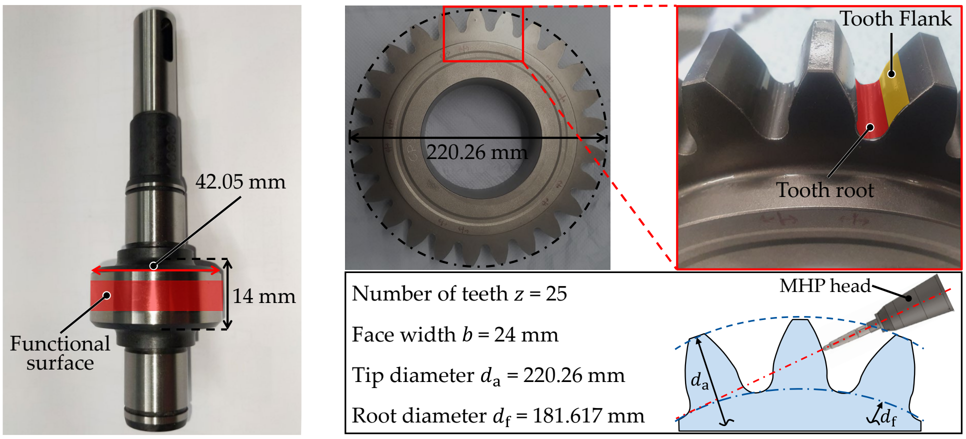

(**a**) (**b**)

Figure 2. (**a**) Cylindrical analog shaft used for initial MHP investigations; (**b**) Real spur gear highlighting critical tooth flank and tooth root regions with limited accessibility for MHP.

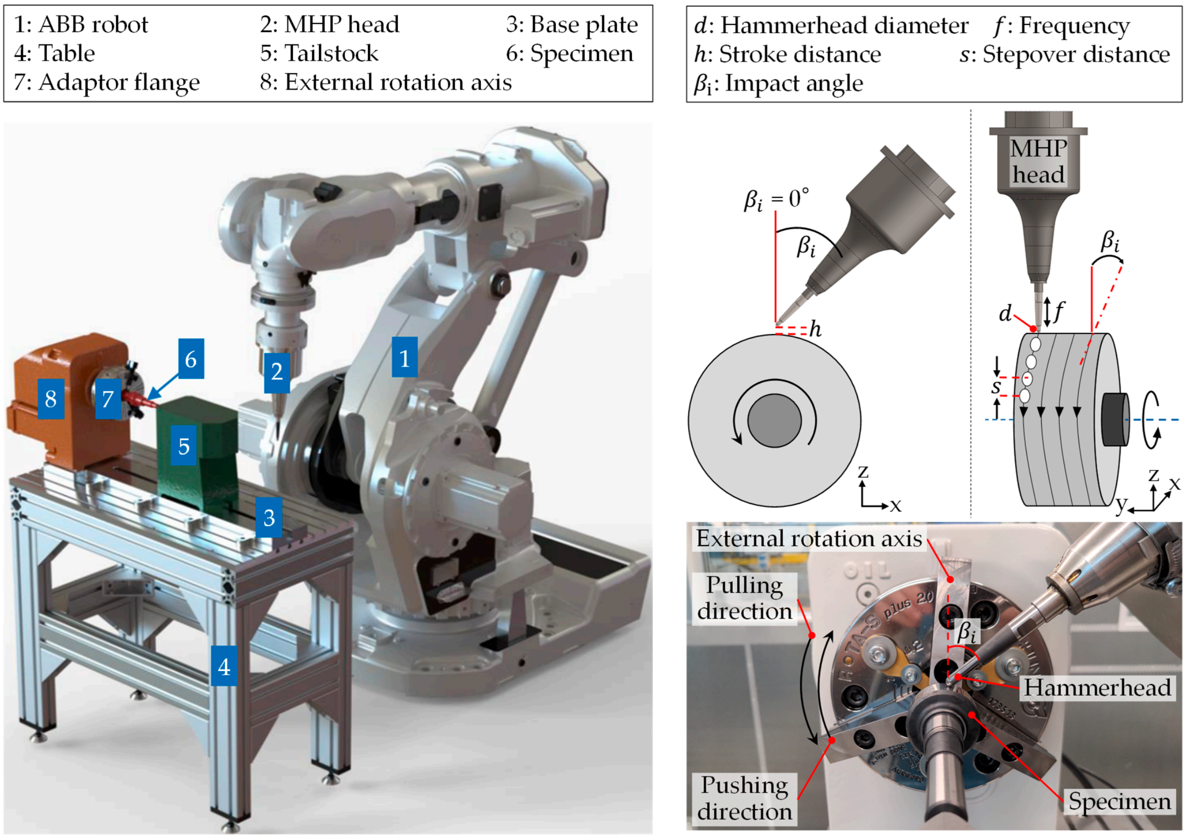

(**a**) (**b**)

Figure 3. (**a**) MHP experimental setup; (**b**) Spiral-like MHP strategy and machining directions.

Table 1. Overview of the experimental settings for the MHP tests.

Frequency f	Stepover Distance s	Stroke Distance h	Hammerhead Diameter d	MHP Impact Angle β_i	MHP Direction
120 Hz	0.07 mm	0.3 mm	8 mm	−15	Pushing
120 Hz	0.07 mm	0.3 mm	8 mm	+15	Pulling
120 Hz	0.07 mm	0.3 mm	8 mm	−30	Pushing
120 Hz	0.07 mm	0.3 mm	8 mm	+30	Pulling
120 Hz	0.07 mm	0.3 mm	8 mm	−45	Pushing
120 Hz	0.07 mm	0.3 mm	8 mm	+45	Pulling

To evaluate the effects of MHP under application-relevant conditions, the manufactured spur gears with 25 teeth and a module of 8 mm were tested. The regions that are difficult to access with MHP are the tooth root and the tooth flank near the root, which are highlighted in Figure 4a. To avoid collisions between the hammer tappet and the gears during MHP and to optimize the complex path planning, offline programming was carried out prior to the experiments. This was done in ABB RobotStudio by simulating the MHP process on the gears and separating the critical areas into distinct machining zones to enable suitable path planning and impact angles for each zone, as shown in Figure 4b. MHP was then applied selectively to the tooth flank and tooth root, which are expected to face the highest operational loads. This selective machining strategy aimed to increase gear load-carrying capacity of the gears while minimizing unnecessary processing.

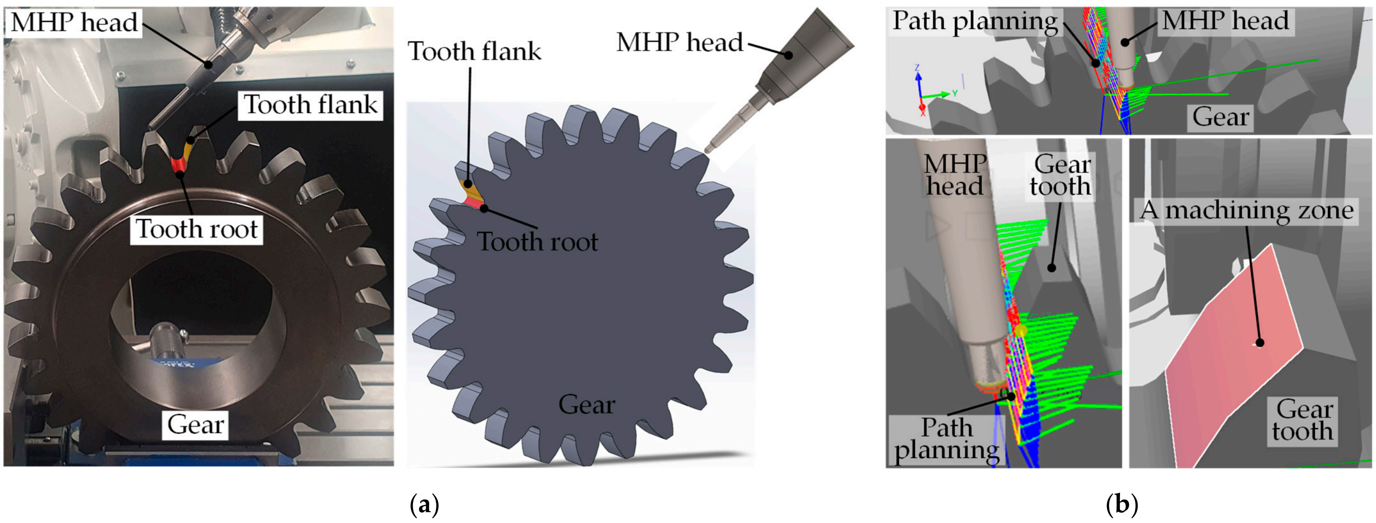

Figure 4. (**a**) Spur gear and the critical functional areas; (**b**) Offline programmed path planning and machining zones created in ABB RobotStudio to enable collision-free MHP processing.

Extra specimens, both analog shafts and real spur gears, were also subjected to controlled shot peening using established industrial parameters for gear components to serve as a reference for a conventional finishing method. Surface integrity characteristics and load-carrying capacity of the specimens in their initial state, after MHP, and after shot peening were measured to analyze the influence of both processes and to compare their modifications. Roughness of the specimens was measured via tactile 2D geometry scans, using a Hommel-Etamic nanoscan 855 contour and roughness measuring device (JENOPTIK Industrial Metrology, Jena, Germany). The measurements had a resolution of 0.5 µm and a probe tip rounding of 2 µm, with three measurements performed at different locations per specimen, following DIN EN ISO 4287 [34] and VDI 2612-5 [35]. Hardness measurements were carried out with the Vickers hardness test according to DIN EN ISO 6507 [36]. For macro hardness, five individual Vickers measurements, using a Zwick ZHU250CL hardness tester (ZwickRoell GmbH & Co. KG, Ulm, Germany), were obtained from the surface of each specimen and averaged. Microhardness measurements were conducted on cross-sections of specimens, using a QNESS 60 A+ EVO microhardness tester (QATM, Vienna, Austria), to assess hardness profiles, with four measurements at each depth and averaged. Residual stress was analyzed via X-ray diffraction (XRD), using a Stresstech diffractometer, to determine the depth profile of tangential residual stresses. For microstructural analysis, cross-sections were examined by Zeiss Axio Imager M2m optical microscopy and ZEISS Sigma 500 VP scanning electron microscopy (SEM) with Gemini Optik (Carl Zeiss AG, Oberkochen, Germany). For the load-carrying capacity analysis, the rolling contact fatigue strength of the tooth flank was determined using a Disk-on-Disk fatigue test rig. The tooth root load-carrying capacity was evaluated using a Schenk PHT 010N pulsator test rig (Schenk Testing Systems, Großostheim, Germany) based on the staircase method.

3. Results

The experimental investigations on case-hardened components provide a detailed understanding of how the MHP process affects surface integrity and mechanical performance relevant to gear applications. The findings are presented in two parts. First, the effects of MHP on surface integrity are examined for both analog specimens and real spur gears. Second, the influence of MHP on the load-carrying capacity of gear-relevant contacts is analyzed.

3.1. Surface Integrity Analysis

This section focuses on the modifications induced by MHP in key surface integrity characteristics of the specimens. The analyses include surface roughness, hardness, and residual stress profiles, which together determine the tribological behavior and fatigue performance of the treated specimens.

3.1.1. Roughness

The influence of MHP on the surface roughness of the analog shafts was significant, with a marked reduction compared to the initial state. This reduction can be attributed to the uniform refinement of the surface by MHP-induced stresses that exceeded the yield strength of the material, leading to plastic deformation. As shown in Figure 5a, both the arithmetic average roughness *Ra* and the average maximum height *Rz* were significantly reduced after MHP. Smaller impact angles β_i resulted in a greater reduction in roughness. At an impact angle of $\beta_i = -15°$, *Ra* decreased from 0.1033 µm in the initial state to 0.0467 µm after MHP, corresponding to a reduction of approximately 55%, while *Rz* decreased from 0.7367 µm to 0.3667 µm at an impact angle of $\beta_i = +15°$, corresponding to a reduction of approximately 50% relative to the initial state. These results indicate that more perpendicular impact angles enable higher energy transfer between the hammer and the workpiece, resulting in higher MHP-induced stresses and greater plastic deformation. It was also observed that the machining direction, whether pushing or pulling, had no significant effect on surface roughness. In comparison, surface roughness increased after shot peening, with *Ra* rising to 0.2133 µm, corresponding to an increase of about 106%, and *Rz* increasing to 1.5367 µm, corresponding to an increase of about 109% compared to the initial state. This difference highlights that MHP primarily smooths and refines the surface due to its systematic and controlled strengthening process, whereas shot peening tends to roughen the surface because it is a random and stochastic strengthening process.

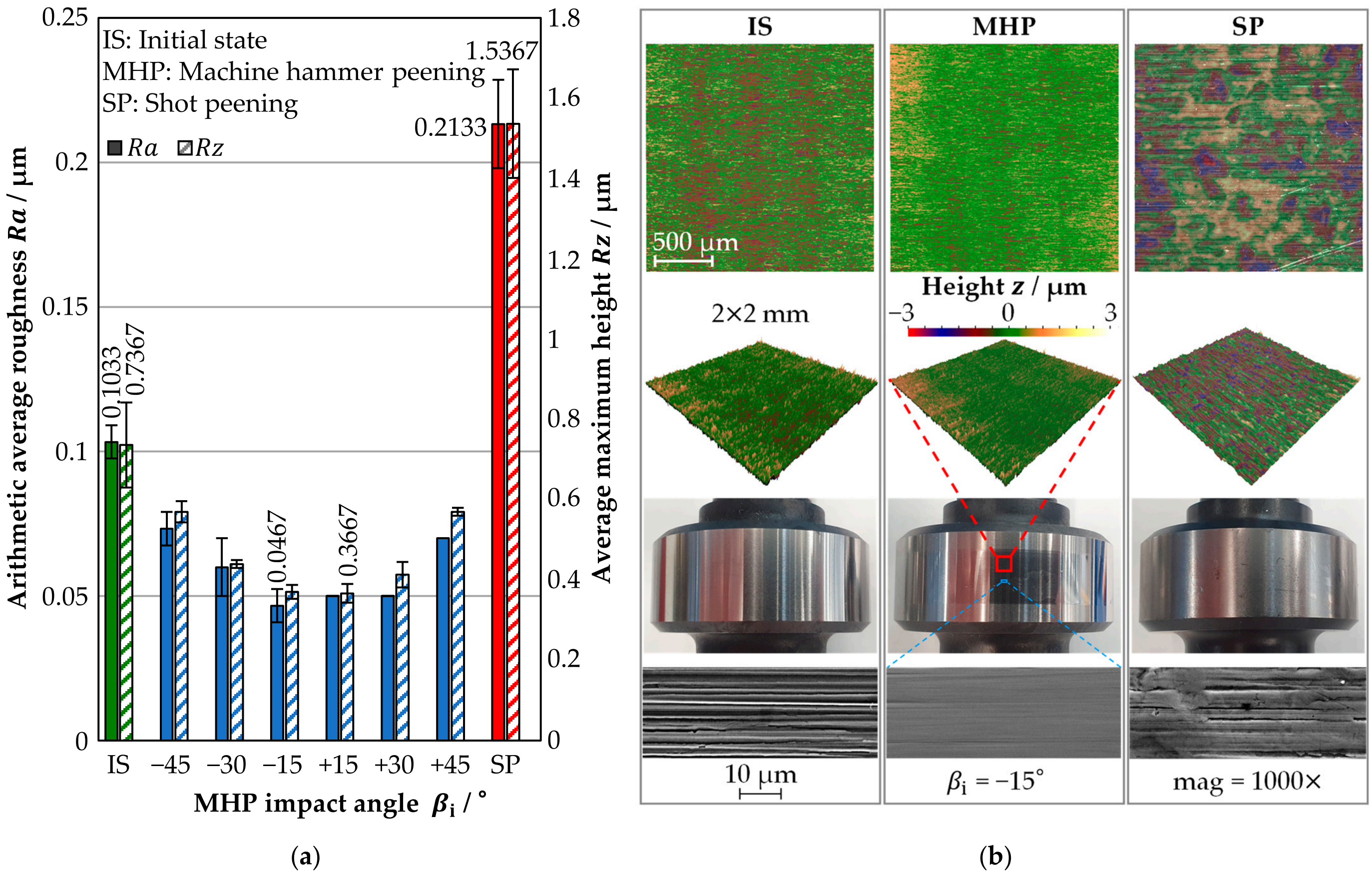

Figure 5. (**a**) Surface roughness *Ra* and *Rz* of the analog shaft specimens in the initial state and after shot peening and MHP at different impact angles; (**b**) 2D/3D surface morphology and SEM images of the specimens.

The above observations are further supported by the topography analysis of the specimens. Figure 5b shows 2D/3D surface profiles and SEM images before and after MHP at an impact angle of $\beta_i = -15°$, which produced the greatest reduction in surface roughness, as well as after shot peening. The surface profiles clearly reveal the finer surface structure obtained after MHP and confirm the uniform refinement generated by the process, which is essential for enhancing the functional performance and service life of the workpiece. The SEM images highlight the pronounced smoothing effect of MHP, caused by plastic deformation within the surface grooves as the applied stresses exceed the yield strength of the material. This results in a more refined and smoother finish. The remaining grooves visible after MHP are remnants of the previous machining process.

The influence of MHP on the surface roughness of the reals spur gears was also evaluated, as shown in Figure 6a. The measurements were conducted at the tooth root of the spur gears, as illustrated in Figure 6b. Compared to the tooth flank analog specimens, the higher roughness levels can be attributed to the different initial surface conditions, since the real gears were examined in the milled state rather than after grinding. Nevertheless, MHP led to a pronounced reduction in the arithmetic average roughness *Ra*, while the influence on the average maximum height *Rz* was lower due to the discrete and localized nature of the hammer impacts, which primarily smooths the general asperity population, whereas isolated peak-to-valley extremes, often associated with machining grooves, are only partially modified due to finite impact overlap. This behavior is consistent with the results obtained for the analog specimens and confirms the smoothing effect of MHP under realistic gear geometries. However, in real spur gears, the difference between the MHP influence on *Ra* and *Rz* is more pronounced due to local accessibility constraints, varying impact angles, and machining direction effects in the tooth root region. Shot peening also resulted in a reduction of *Ra* at the tooth root. However, the resulting reduction was smaller than that obtained by MHP. Similar to the analog specimens, shot peening caused an increase in *Rz* compared to the initial state, because localized indentations and material pile-up generated by individual shot impacts can increase isolated peak-to-valley distances, even though the overall surface roughness level reflected by *Ra* is reduced. This increase was accompanied by considerable measurement scatter, which can be attributed to the stochastic nature of shot peening.

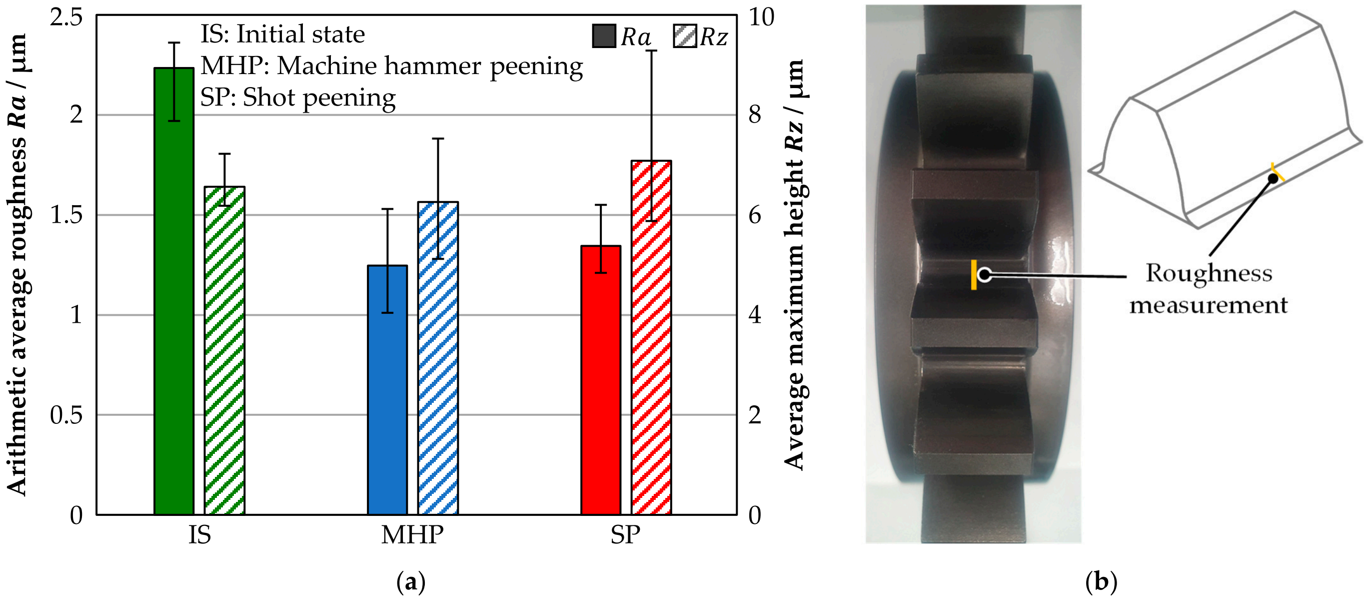

Figure 6. (**a**) Surface roughness *Ra* and *Rz* of the tooth root of real spur gears in the initial state and after shot peening and MHP; (**b**) Location of the surface roughness measurements at the tooth root of a real spur gear.

3.1.2. Hardness

Both macro hardness and microhardness measurements were conducted on the specimens. Macro hardness was evaluated at the surface, while microhardness was assessed at selected depths to characterize the hardness depth profile. As shown in Figure 7a, MHP treatment resulted in a significant increase in surface hardness, with a more pronounced effect observed at smaller impact angles. This indicates that nearly perpendicular impact angles enhance the effectiveness of MHP in increasing hardness, as higher energy is transferred to the specimen, leading to increased work hardening. The highest surface hardness after MHP was achieved at an impact angle of β_i= +15°, reaching *HV* = 846 HV30, which corresponds to an increase of more than 30% compared to the initial value of *HV* = 648 HV30. The machining direction of the MHP process had no significant influence on hardness, consistent with the trend observed for surface roughness. In comparison, shot peening also led to an increase in surface hardness, reaching *HV* = 698 HV30, which corresponds to an increase of less than 8% relative to the initial state. However, this increase was clearly lower than that achieved by MHP, even when MHP was applied at the highest impact angle. In addition, the scatter of measured hardness values for each MHP condition was significantly narrower than that observed for shot peening. This uniformity demonstrates that MHP produces a more consistent and controlled surface modification, whereas shot peening yields larger variability due to its stochastic impact mechanism. The comparatively inconsistent hardness increase associated with shot peening further highlights the advantages of MHP in delivering more reliable and repeatable surface hardening, which is crucial for the long-term performance of gear components.

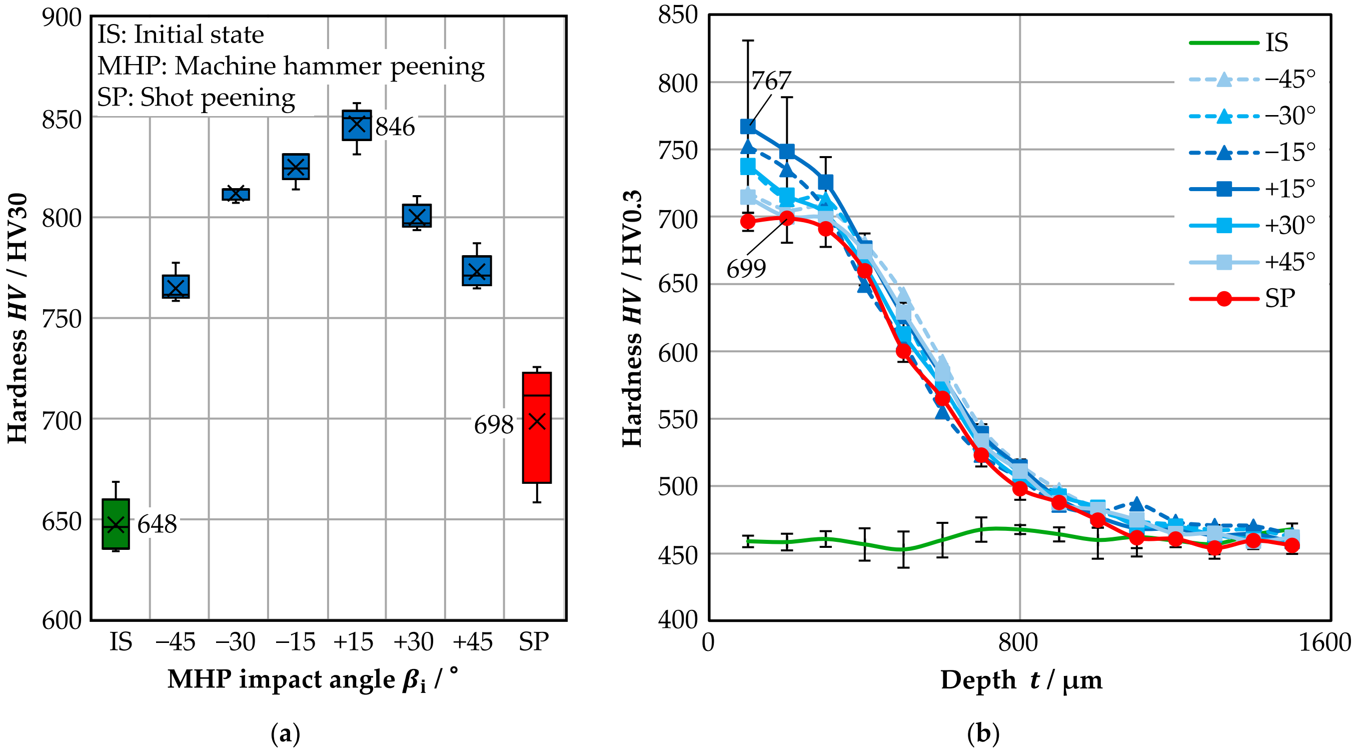

Figure 7. (**a**) Surface macro hardness *HV* of the specimens in the initial state and after shot peening and MHP at different impact angles; (**b**) Microhardness depth profile of the specimens.

Figure 7b shows the measured microhardness for the MHP-treated and shot-peened specimens. Overall, the observations for microhardness are consistent with those for macro hardness and confirm the general trends. Both MHP and shot peening increase hardness, with the strongest effect observed for MHP at smaller impact angles. As with the macro hardness results, no significant influence of the MHP direction was found. The highest microhardness values occurred near the surface, where the highest energy is transferred, resulting in maximum work hardening. For MHP, the highest value was HV = 767 HV0.3 at an impact angle of β_i = +15°, while the highest hardness achieved by shot peening was HV = 699 HV0.3. These values follow the same trend as the surface macro hardness values shown in Figure 7a. The hardness increase extends to a depth of approximately t = 1000 µm, after which the values converge toward the initial hardness of the untreated specimen, around HV= 460 HV0.3. The measured microhardness of the untreated specimen differs from the macro hardness values due to methodological differences. Microhardness is measured in a smaller, localized area and is more sensitive to microstructural variations, while macro hardness provides an average value over a larger area. Before treatment, the microstructure is less homogeneous, which leads to discrepancies between the two methods. After treatment, significant work hardening and surface modification result in a more homogeneous microstructure, so that both methods yield similar results.

3.1.3. Residual Stresses

Figure 8a shows that MHP induced high compressive residual stresses, whereas no tensile residual stresses were present after MHP. The mechanism behind this residual stress induction is attributed to plastic deformation and stress redistribution as a result of MHP. Here, too, smaller impact angles led to higher energy transfer, which ultimately resulted in higher residual compressive stresses. The MHP direction had no significant influence on the induced residual stresses. The highest compressive residual stresses were achieved at an impact angle of β_i = +15°, with σ_{RS} exceeding −1400 MPa and extending over a depth greater than t = 200 µm. In comparison, shot peening induced compressive residual stresses only in the surface and near-surface zone, with a shallower depth and lower magnitude. Although the peak values introduced by shot peening were lower than those of MHP at lower impact angles, it exhibited the strongest near-surface compressive stress field. In contrast, the MHP-treated specimens developed a much deeper compressive stress zone due to the intense plastic deformation and enlarged affected volume.

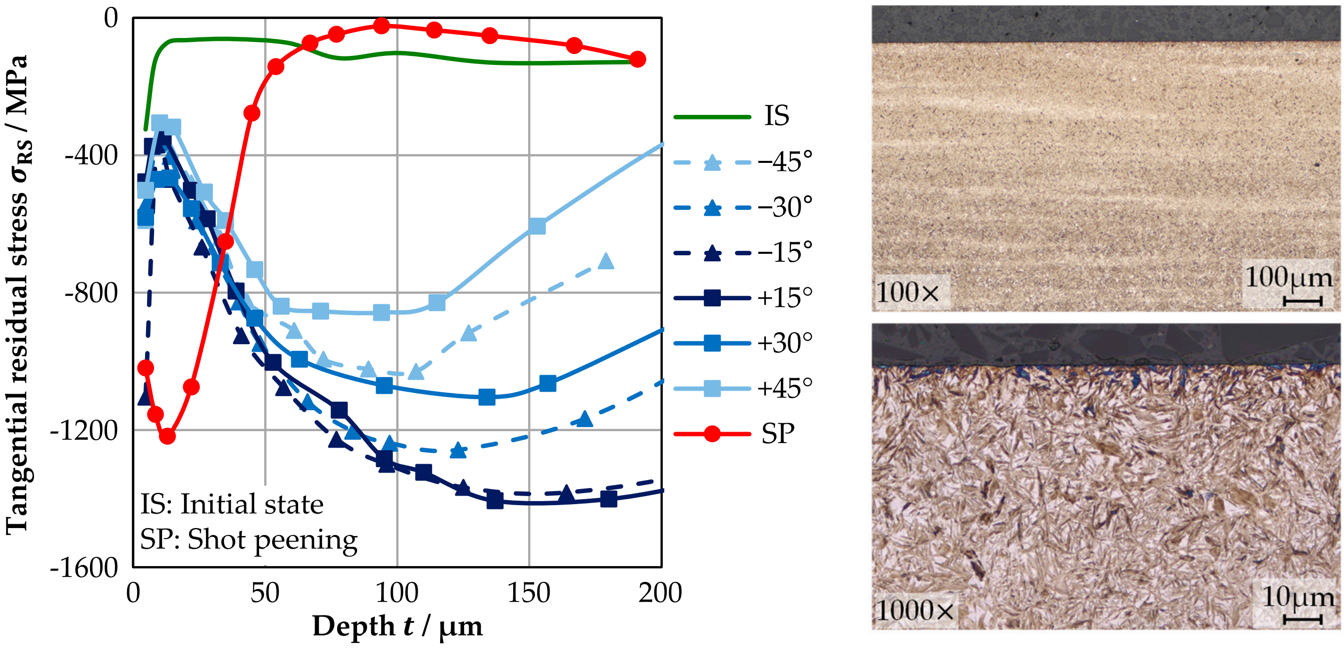

(**a**) (**b**)

Figure 8. (**a**) Residual stresses σ_{RS} of the analog shaft specimens in the initial state and after shot peening and MHP at different impact angles; (**b**) Optical microscopic cross-sectional images of the hammered specimen.

This deep material hardening was so pronounced that it was necessary to investigate whether microcracks had formed on the surface of the specimens. As shown in Figure 8b, optical microscopic cross-sectional images of the specimen with the highest compressive residual stresses, treated with MHP at an impact angle β_i = +15°, revealed that no microcracks were present. This demonstrates that MHP can increase fatigue strength by inducing deep compressive residual stresses without causing surface damage. This represents a significant advantage over conventional shot peening, where compressive stresses typically penetrate only shallow depths.

The influence of MHP on the residual stress state of real spur gears was additionally evaluated at the tooth root, as shown in Figure 9. After MHP, the tooth root exhibited a pronounced increase in compressive residual stresses, with σ_{RS} exceeding −1100 MPa and extending over a depth greater than t = 200 µm. In comparison, shot peening also generated compressive residual stresses at the tooth root, but with lower magnitude. This highlights the effectiveness of localized MHP treatment in generating deep and pronounced compressive residual stresses even in geometrically restricted regions. However, compared to the residual stress profiles obtained for the analog specimens, the maximum compressive residual stresses induced by MHP in the tooth root were lower, reflecting the reduced

MHP effectiveness under geometrical constraints. Overall, these results demonstrate that selective MHP application at the tooth root enables the introduction of compressive residual stresses, which are particularly advantageous for enhancing fatigue resistance in critical load-bearing regions of real spur gears.

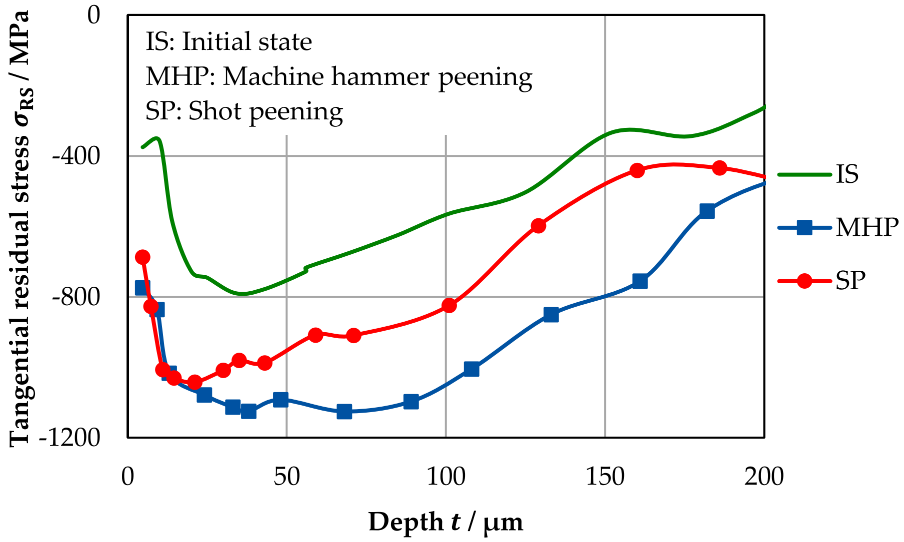

Figure 9. Residual stresses σ_{RS} at the tooth root of real spur gears in the initial state and after shot peening and MHP.

3.2. Load-Carrying Capacity Analysis

This section investigates the influence of MHP on the load-carrying capacity of gear-relevant contacts under fatigue loading. The load-carrying behavior is evaluated using fatigue tests on tooth flank analog specimens and on the tooth root of real spur gears, representing different failure-critical regions in spur gears. This approach allows the effects of surface finishing on load-carrying capacity to be assessed under both simplified test conditions and tests on real spur gears.

First, the influence of surface finishing on the load carrying-capacity of tooth flank analog specimens was examined. Figure 10 shows the mean number of load cycles to failure out of 3 tests for all investigated variants. The untreated specimen in the initial state reached a mean load cycle number of N_L = 1.23 × 10^6, which increased to N_L = 2.45 × 10^6 for the MHP-treated specimen with an impact angle of β_i = +15°, corresponding to an increase of more than 99%. For MHP in the pulling direction, higher impact angles led to a smaller increase in fatigue life, with β_i = +45° exhibiting the lowest load cycle number within this group. In contrast, for MHP in the pushing direction, fatigue strength increased with increasing impact angle, as β_i = −45° exhibited the highest load cycle number in this group. Notably, the configuration with β_i = −15° even showed a slightly lower fatigue strength than the untreated specimen. This directional dependence of the MHP effect on fatigue differs from the trends observed for surface integrity, where the MHP direction had no significant influence. These results indicate that rolling-sliding contact fatigue performance is governed by an interplay between the depth and magnitude of compressive residual stresses and the orientation and amplitude of surface features relative to the rolling direction. Compared with all MHP-treated variants, the shot-peened specimen exhibited by far the highest rolling-contact fatigue strength, reaching a mean load cycle number of N_L = 16 × 10^6. This superior performance can be attributed to the strong near-surface compressive residual stress field generated by shot peening, which is highly effective in delaying crack initiation despite the increased surface roughness resulting from shot peening.

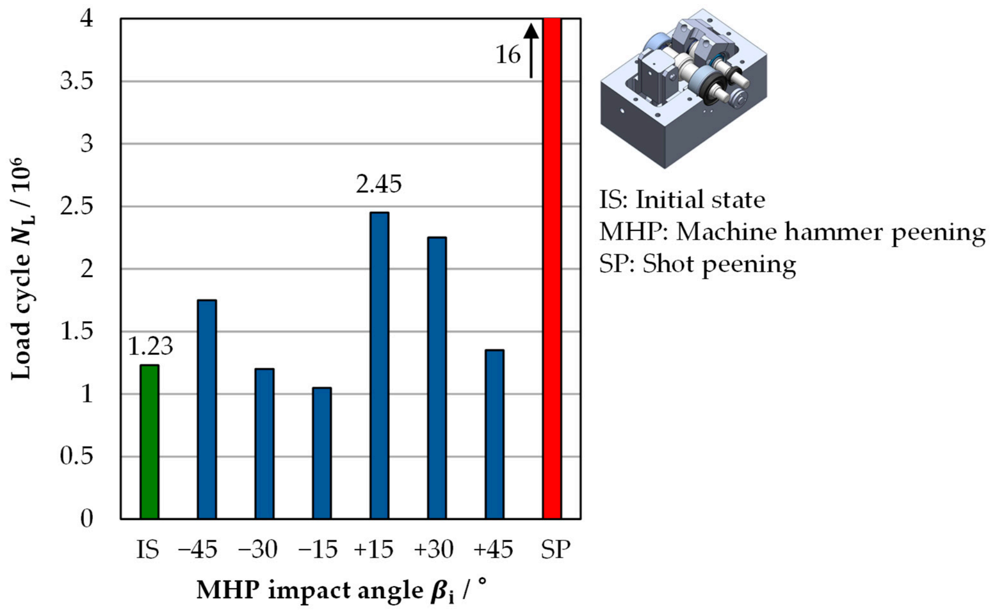

Figure 10. Mean numbers of load cycles of tooth flank analog specimens in the initial state and after shot peening and MHP at different impact angles.

The difference in performance between MHP-treated and shot-peened specimens became more pronounced in real spur gears. While the analogy tests revealed a clear fatigue-strength advantage for the shot-peened condition, this trend could be confirmed in tooth root test on real spur gears, where MHP could not be applied uniformly to all critical load-carrying regions. Complex geometrical features, such as varying curvature and limited accessibility in the tooth root area, restricted the hammering tool from achieving consistent impact angles and complete surface coverage. As a result, the beneficial near-surface compressive residual stresses and surface modifications induced by MHP remained more localized and less homogeneous than in the simplified analogy specimens. Figure 11 illustrates the influence of surface finishing on the load carrying-capacity of the tooth root of real spur gears, showing that, despite these limitations, MHP increased the average double amplitude by 5.6% compared to the initial state, whereas shot peening resulted in a higher increase of 23.4%. For both MHP-treated and shot-peened specimens, the number of load cycles to failure ranged between 0.2 × 10^6 and 0.5 × 10^6 load cycles.

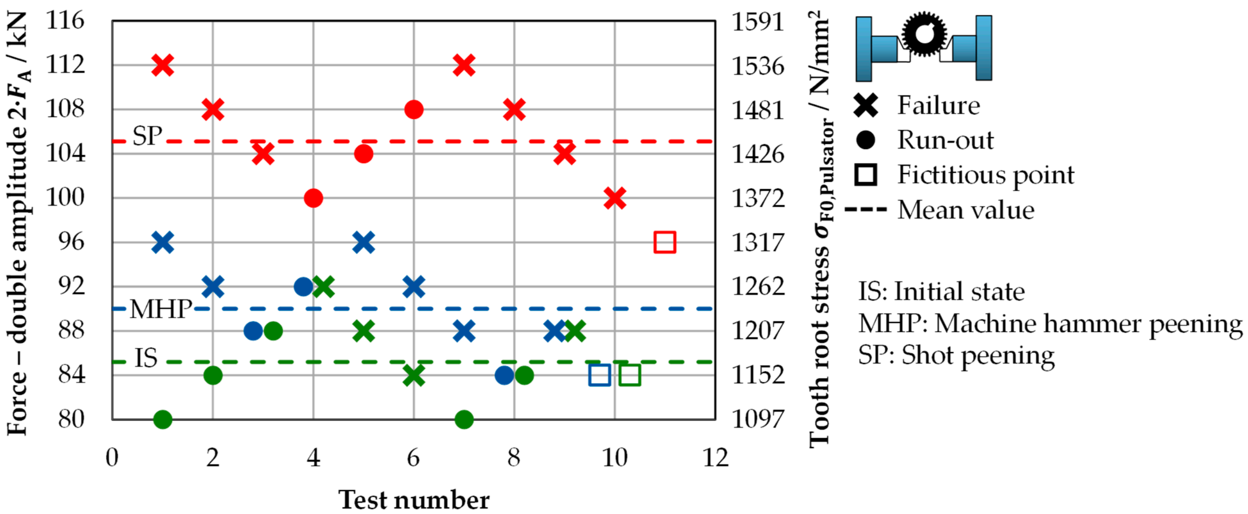

Figure 11. Staircase method results for tooth root load-carrying capacity of real spur gears in the initial state and after shot peening and MHP.

Overall, these results demonstrate that while MHP can enhance the load-carrying capacity of both the tooth flank and tooth root, shot peening remains more effective for real spur gears. This superiority is attributed to the strong near-surface compressive residual stress field generated by shot peening and the absence of accessibility limitations, resulting in a more favorable residual-stress state and surface condition along the entire load path. For the tooth flank, the findings indicate that the effectiveness of MHP is strongly influenced by the processing direction relative to the local rolling–sliding motion. Treatments aligned with the local sliding direction promote a favorable orientation of MHP-induced surface structures and residual stresses, which contributes to increased rolling–sliding contact fatigue strength. This directional effect depends on the functional role of the gear, as different loading directions along the flank occur for driving and driven gears, as schematically illustrated in Figure 12. In contrast, in the tooth root region, which is highly notch-sensitive and dominated by radial stresses, the processing direction plays a subordinate role. Here, the load-carrying capacity is governed primarily by the local energy input, enabling targeted plastic deformation and compressive residual stress induction without increasing the risk of surface damage due to excessive single impacts. Consequently, the results highlight that the load-carrying performance achieved by MHP is controlled by a location-dependent interplay between accessibility, residual stress state, and process kinematics, which becomes particularly critical under realistic gear geometries. Thus, in real spur gears, where complete and uniform surface treatment is essential for maximizing load-carrying capacity, the superiority of shot peening over MHP becomes particularly evident.

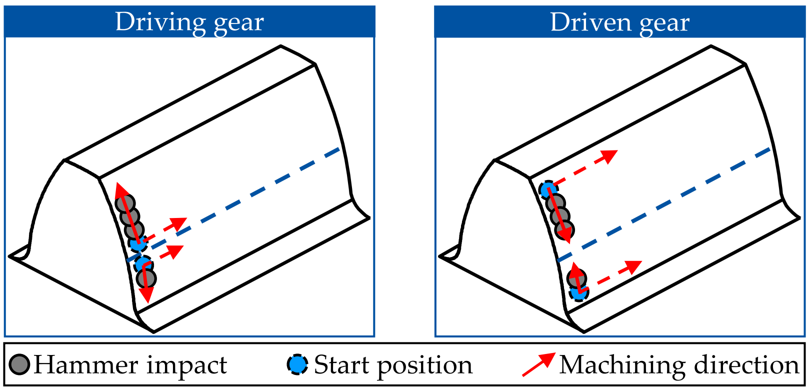

Figure 12. MHP machining direction on the tooth flank for driving and driven spur gears.

4. Discussion

The present study confirms that MHP is capable of substantially modifying the surface integrity of case-hardened gear components. However, beyond the observed improvements in roughness, hardness, and residual stress state, the results demonstrate that the effectiveness of MHP is strongly governed by geometric accessibility and impact angle control, which become critical factors in real gear geometries, particularly when functional active tooth flank areas must be treated under constrained kinematic conditions.

The comparison between analog shafts and real spur gears highlights a key distinction between process capability and process applicability. On geometrically simple specimens, where MHP can be applied with uniform coverage and near-perpendicular impact angles, the process generates smooth surfaces, consistent hardening, and deep compressive residual stresses that are generally favorable for fatigue resistance over a wide range of operating conditions. In contrast, for real gears, curved tooth flanks and deep root regions combined with the limited spacing between adjacent gear teeth restrict tool accessibility and prevent the hammerhead from maintaining optimal impact orientations throughout the entire contact path. As a result, the induced surface modifications remain localized and less homogeneous, which limits their effectiveness under rolling-contact fatigue conditions, especially in regions subjected to high cyclic stress amplitudes.

The comparison between tooth root and tooth flank responses highlights the location-dependent nature of MHP effectiveness and underscores the importance of selective surface modification. In the tooth root region, which is highly notch-sensitive, the load-carrying capacity is governed primarily by the local energy input. Accordingly, the MHP energy density emerges as a key control parameter, determined by the combined interaction of stroke distance, impact angle, and stepover distance. These parameters define the local energy input and the resulting plastic deformation, which constitutes the primary strengthening mechanism and leads to increased surface hardness and compressive residual stresses that contribute to improved fatigue performance. In contrast, for the tooth flank, the effectiveness of MHP is strongly influenced by the processing direction relative to the local rolling–sliding motion. Treatments aligned with the sliding direction promote a favorable orientation of MHP-induced surface structures and residual stresses, thereby enhancing rolling–sliding contact fatigue strength. The results further indicate that deep compressive residual stresses alone are not sufficient to ensure superior fatigue performance. Instead, fatigue behavior is governed by a balance between residual stress depth, near-surface stress magnitude, and the uniformity of the modified surface layer along the load path. Under realistic gear geometries, this balance is strongly affected by accessibility and process kinematics, which limit the homogeneity of MHP-induced modifications. Consequently, in real spur gears, where complete and uniform surface treatment is essential for maximizing load-carrying capacity, shot peening remains more effective. This is attributed to its ability to uniformly treat complex geometries and to generate a pronounced near-surface compressive residual stress field, which is more effective in delaying crack initiation under rolling contact and repeated cyclic loading.

These findings underline that, for components with complex geometries, accessibility and treatment uniformity can outweigh the intrinsic strengthening capability of a surface treatment process. Accordingly, MHP is best suited for applications involving simple or well-accessible surfaces, or where targeted and localized strengthening is required to address specific functional zones. For industrial gear applications, further developments in tool kinematics, automated path planning, and hybrid processing strategies are necessary to fully exploit the potential advantages of MHP, while ensuring sufficient coverage and process robustness in geometrically constrained regions.

To verify that the shot peening reference condition applied in this study is representative, the obtained results were compared with published data on shot-peened gears. Literature reports arithmetic average roughness values after shot peening in the range of around 0.2 μm for comparable industrial applications [37], which is consistent with the surface condition achieved in the present work. Reported near-surface microhardness values of about 770 HV0.3 [38] and compressive residual stresses exceeding −1200 MPa [39] together with a comparable depth of effect, are likewise in good agreement with the state obtained here. Furthermore, previous investigations have demonstrated increases in load-carrying capacity of approximately 20% after shot peening [40], which aligns well with the improvements observed in this study. These comparisons confirm that the applied shot peening parameters resulted in a typical and practically relevant surface condition, thereby providing a reliable benchmark for evaluating the effectiveness of MHP.

In addition to the technical advantages and limitations discussed above, environmental and economic aspects should also be considered when comparing MHP and shot peening. A fundamental difference between the two processes lies in the use of consumable media. Shot peening requires blasting media that must be supplied, collected, cleaned, and periodically replaced, increasing material handling, logistics effort, and potential waste generation. In contrast, MHP operates without consumable media and can be integrated directly into machining centers, reducing the need for separate processing steps. Moreover, MHP enables highly localized surface modification through direct tool-based energy input, whereas localized shot peening typically requires masking techniques involving auxiliary materials and additional effort. Consequently, for suitable geometries and applications, MHP may offer advantages in terms of reduced material consumption, simplified process chains, and potentially lower environmental impact.

5. Conclusions

MHP demonstrates clear potential as a finishing process for improving the surface integrity and load-carrying capacity of spur gears. However, its applicability to complex gear geometries remains limited due to accessibility constraints. The main conclusions of this study are as follows:

- MHP effectively enhances surface integrity by reducing the arithmetic average roughness from 0.1033 μm up to 0.0467 μm in analog shaft and from 2.2333 μm to 1.2465 μm in spur gears, increasing surface macro hardness from 648 HV30 up to 846 HV30, increasing near-surface microhardness from approximately 460 HV0.3 up to 767 HV0.3, and inducing deep compressive residual stresses that extend to depths greater than 200 μm and exceed −1400 MPa in analog shafts and −1100 MPa in spur gears;
- Impact angles close to perpendicular result in the strongest modifications in surface integrity characteristics;
- The machining direction during MHP, whether pushing or pulling, does not significantly influence the surface integrity outcomes, but shows an influence on the rolling-sliding contact fatigue strength;
- For simple or well-accessible geometries, MHP offers clear advantages over shot peening due to its controllability and its ability to generate deeper strengthening effects;
- MHP increases fatigue strength when an optimal and stable impact orientation is maintained, increasing the number of load cycles to failure for tooth flanks from 1.23×10^6 up to 2.45×10^6, while increasing the average double amplitude from 85.2 kN to 90 kN, with the number of load cycles to failure for tooth root ranging between 0.2×10^6 and 0.5×10^6;
- Shot peening produces higher load-carrying capacity than MHP because of its superior accessibility and higher near-surface stress field, resulting in a mean load cycle number of 16×10^6 for tooth flank and an increase of 23.4% in the average double amplitude for tooth root.

Future research directions stemming from this study, mainly based on the gained knowledge regarding the advantages and limitations of MHP for gear applications, can be summarized as follows:

- Improving MHP tool accessibility through optimized tappet design and advanced path-planning strategies to better accommodate complex tooth geometries;
- Investigating hybrid surface finishing concepts that combine MHP with shot peening or other finishing processes to balance strengthening depth with surface uniformity.

Author Contributions: Conceptualization, T.H., D.M., C.B. and T.B.; methodology, T.H., M.M., D.M. and R.G.; validation, S.S. and M.D.; formal analysis, S.S. and M.D.; investigation, S.S., R.G. and M.D.; resources, T.B. and C.B.; writing—original draft preparation, M.D.; writing—review and editing, M.M., S.S. and T.H.; supervision, M.M., T.H. and R.G.; project administration, T.H.; funding acquisition, T.B. All authors have read and agreed to the published version of the manuscript.

Funding: This research was funded by the Deutsche Forschungsgemeinschaft (DFG, German Research Foundation), project number: 390969378.

Data Availability Statement: The original contributions presented in this study are included in the article. Further inquiries can be directed to the corresponding author.

Acknowledgments: The authors gratefully acknowledge Curtiss-Wright Metal Improvement Company, LLC, Werk Unna, for performing the shot peening treatments used in this study. Their technical support contributed to the successful completion of the experimental work.

Conflicts of Interest: The authors declare no conflicts of interest.

Abbreviations

The following abbreviations are used in this manuscript:

IS	Initial State
MHP	Machine Hammer Peening
SP	Shot Peening
SEM	Scanning Electron Microscopy
XRD	X-ray Diffraction

References

1. Li, F.; Ding, N.; Song, M.; Zhong, Z.; Liu, L.; Shen, X.; Xu, H.; Tian, L.; Xu, N.; Guo, W.; et al. A Review on Research of Gear Failures in Mechanical Equipment. *J. Fail. Anal. Prev.* **2025**, *25*, 612–648. [CrossRef]
2. Deutsches Institut für Normung. *DIN 3979: Zahnschäden an Zahnradgetrieben*; Bezeichnung, Merkmale, Ursachen; DIN Media GmbH: Berlin, Germany, 1979.
3. Starzhinskii, V.E.; Soliterman, Y.L.; Goman, A.M.; Osipenko, S.A. Forms of damage to gear wheels: Typology and recommendations on prevention. *J. Frict. Wear* **2008**, *29*, 340–353. [CrossRef]
4. Uhlmann, L. Optimization of the Application Behavior of Spur Gears by Means of Machine Hammered Tooth Surfaces. Master's Thesis, RWTH Aachen University, Aachen, Germany, 2019.
5. Klocke, F.; Brecher, C. *Zahnrad- und Getriebetechnik: Auslegung—Herstellung—Untersuchung—Simulation*; Carl Hanser Verlag: München, Germany, 2017.
6. Zhao, J.; Tang, J.; Zhou, W.; Jiang, T.; Wu, H.; Liao, X.; Guo, M. Surface integrity of gear shot peening considering complex geometric conditions: A sequential coupled DEM-FEM method. *Surf. Coat. Technol.* **2022**, *449*, 128943. [CrossRef]
7. Kratzer, D.; Koller, P.; Tobie, T.; Stahl, K. Investigation of the effects of surface roughness and shot peening on the tooth root bending strength of case-carburized gears. *J. Mech. Sci. Technol.* **2022**, *36*, 731–740. [CrossRef]
8. Wang, G.; Sang, X.; Wang, S.; Zhang, Y.; Xu, G.; Zhao, M.; Peng, Z. Surface integrity and corrosion resistance of 18CrNiMo7-6 gear steel subjected to combined carburized treatment and wet shot peening. *Surf. Coat. Technol.* **2024**, *484*, 130862. [CrossRef]
9. Cermak, H.; Tobie, T.; Stahl, K. Flame and Induction Hardening—An Advantageous Alternative to Case Hardening for Large Size Gears? *HTM J. Heat Treat. Mater.* **2022**, *77*, 112–126. [CrossRef]
10. ENRX. Induction Hardening for Enhanced Steel Durability. 2025. Available online: https://www.enrx.com/en/Induction-Applications/Induction-heating-applications/Hardening (accessed on 18 December 2025).
11. Radzevich, S.P. *Dudley's Handbook of Practical Gear Design and Manufacture*; CRC Press: Boca Raton, FL, USA, 2012.
12. Zhang, B.; Sun, L.; Zhao, N.; Li, J. Applications of Laser Surface Treatment in Gears: A Review. *J. Mater. Eng. Perform.* **2025**, *34*, 1–35. [CrossRef]
13. Stahl, K.; Höhn, B.-R.; Michaelis, K.; Hinterstoisser, M.; Mayer, J. (Eds.) Influence of Surface Texture and Coating on the Coefficient of Friction in EHL Contacts. In Proceedings of the International Conference on Gears, Garching, Germany, 7–9 October 2013; pp. 969–980.
14. Holmberg, K.; Andersson, P.; Erdemir, A. Global energy consumption due to friction in passenger cars. *Tribol. Int.* **2012**, *47*, 221–234. [CrossRef]
15. Baiocco, G.; Genna, S.; Salvi, D.; Ucciardello, N. Laser Texturing to Increase the Wear Resistance of an Electrophoretic Graphene Coating on Copper Substrates. *Materials* **2023**, *16*, 5359. [CrossRef]
16. Joachim, F.J.; Kurz, N.; Glatthaar, B. Influence of coatings and surface improvements on the lifetime of gears. *Gear Technol.* **2004**, *21*, 50–56.
17. Sundar, R.; Ganesh, P.; Ram Kishor, G.; Ragvendra, G.; Pant, B.K.; Kain, V.; Ranganathan, K.; Kaul, R.; Bindra, K.S. Laser Shock Peening and its Applications: A Review. *Lasers Manuf. Mater. Process.* **2019**, *6*, 424–463. [CrossRef]

18. Liu, H.; Niu, R.; Meng, Y. The Effect of Laser Texturing of Steel Surfaces on Film Lubriction Based on Stribeck Curves. In *Advanced Tribology*; Springer: Berlin/Heidelberg, Germany, 2009; pp. 685–687.
19. Sandmann, P.; Keller, S.; Kashaev, N.; Ghouse, S.; Hooper, P.A.; Klusemann, B.; Davies, C.M. Influence of laser shock peening on the residual stresses in additively manufactured 316L by Laser Powder Bed Fusion: A combined experimental–numerical study. *Addit. Manuf.* **2022**, *60*, 103204. [CrossRef]
20. Dadgar, M.; Gräfe, S.; Müller, M.; Herrig, T.; Bergs, T. Surface Integrity of Additively Manufactured Workpieces after Machine Hammer Peening. *Procedia CIRP* **2024**, *123*, 161–166. [CrossRef]
21. Schulze, V. *Modern Mechanical Surface Treatment*; Wiley-VCH: Weinheim, Germany, 2006.
22. Trauth, D.H. Tribology of Machine Hammer Peened Tool Surfaces for Deep Drawing. Doctoral Dissertation, RWTH Aachen University, Aachen, Germany, 2016.
23. VDI Verein Deutscher Ingenieure e.V. *Maschinelles Oberflächenhämmern: Grundlagen*; VDI: Dusseldorf, Germany, 2019.
24. Bleicher, F.; Lechner, C.; Habersohn, C.; Kozeschnik, E.; Adjassoho, B.; Kaminski, H. Mechanism of surface modification using machine hammer peening technology. *CIRP Ann.* **2012**, *61*, 375–378. [CrossRef]
25. Nie, N.; Yu, L.; Xu, S.; Tian, Q.; Ding, C.; Su, L.; Wang, H. Study on the Morphology, Wear Resistance, and Corrosion Resistance of CuSn12 Alloys Subjected to Machine Hammer Peening. *Metals* **2025**, *15*, 444. [CrossRef]
26. Revilla-Gomez, C.; Buffiere, J.-Y.; Verdu, C.; Peyrac, C.; Daflon, L.; Lefebvre, F. Assessment of the Surface Hardening Effects from Hammer Peening on High Strength Steel. *Procedia Eng.* **2013**, *66*, 150–160. [CrossRef]
27. Liu, Q.; Chen, S.; Xu, X.; Jin, S.; Li, Y.; Wang, Y.; Shen, B. Multi-objective optimization of the subsurface residual stress field of TC4 alloy in machine hammer peening. *J. Manuf. Process.* **2023**, *104*, 98–107. [CrossRef]
28. Mannens, R. Increasing fatigue strength of austenitic stainless steel using machine hammer peening. Doctoral Dissertation, RWTH Aachen University, Aachen, Germany, 2021.
29. Rego, R.; Löpenhaus, C.; Gomes, J.; Klocke, F. Residual stress interaction on gear manufacturing. *J. Mater. Process. Technol.* **2018**, *252*, 249–258. [CrossRef]
30. Bergs, T.; Uhlmann, L.; Mannens, R.; Trauth, D. Inkrementelle Randzonenmodifikation von einsatzgehärteten 16MnCr5-Stirnrädern mittels maschinellem Oberflächenhämmern. *Tribol. Und Schmier.* **2020**, *67*, 7–14.
31. Mevissen, D.; Uhlmann, L.; Brimmers, J.; Herring, T.; Bergs, T. Wälzfestigkeit maschinell gehämmerter Oberflächenstrukturen im Zahnflankenanalogieversuch. *Tribol. Und Schmier.* **2022**, *69*, 34–40. [CrossRef]
32. Dadgar, M.; Greschert, R.; Müller, M.; Sklenak, S.; Herrig, T.; Brimmers, J.; Bergs, T. Effects of machine hammer peening on case-hardened 16MnCr5 gear analogue shafts. *Mater. Form. ESAFORM* **2024**, *41*, 1373–1381.
33. Sklenak, S.; Dadgar, M.; Mevissen, D.; Westphal, C.; Herrig, T.; Brecher, C.; Bergs, T. Experimental investigation of the load-carrying capacity of machine-hammered surfaces with variation of the process parameters. *Tribol. Und Schmier.* **2024**, *71*, 12–18. [CrossRef]
34. *DIN EN ISO 4287*; Geometrische Produktspezifikation (GPS)—Oberflächenbeschaffenheit: Tastschnittverfahren—Benennungen, Definitionen und Kenngrößen der Oberflächenbeschaffenheit, 3rd ed. Beuth: Berlin, Germany, 2010.
35. *VDI-Richtlinie 2612-5*; Measurement and Testing of Gearings Surface Roughness Measurement of Cylindrical Gears and Bevel Gears by Means of Stylus-Type Instruments 2015. VDI Verein Deutscher Ingenieure e.V.: Dusseldorf, Germany, 2015.
36. *DIN EN ISO 6507-1*; Metallische Werkstoffe—Härteprüfung nach Vickers—Teil 1: Prüfverfahren, 2022. Deutsches Institut für Normung: Berlin, Germany, 2022.
37. Jbily, D.; Amar, L.; Simonneau, A. Experimental and analytical study of the effect of shot peening on gear micropitting and contact fatigue failure. *Gear Technol.* **2024**, 43–51.
38. Zhong, Z.; Huang, X.; Zhang, C.; Zou, J.; Zhu, Y.; Liu, X. Experimental study on the bending fatigue characteristics of shot peening gears. *J. Phys. Conf. Ser.* **2025**, *3068*, 12030. [CrossRef]
39. Bretl, N.; Schurer, S.; Tobie, T.; Stahl, K.; Höhn, B.-R. Investigations on Tooth Root Bending Strength of Case Hardened Gears in the Range of High Cycle Fatigue. *Therm. Process. Gear Solut.* **2014**, 52–59.
40. Sorg, A.; Boyraz, M.T.; Tobie, T.; Steinbacher, M.; Stahl, K.; Fechte-Heinen, R. Investigations on the tooth root load-carrying capacity of carbonitrided gears containing high amounts of retained austenite. *Forsch. Ingenieurwes* **2025**, *89*, 124. [CrossRef]